

# Multi-objective optimal design of hybrid renewable energy systems using PSO-simulation based approach



Masoud Sharafi<sup>a</sup>, Tarek Y. ELMekkawy<sup>b,\*</sup>

<sup>a</sup> Department of Mechanical Engineering, University of Manitoba, Winnipeg, MB R3T 5V6, Canada

<sup>b</sup> Department of Mechanical and Industrial Engineering, Qatar University, P.O. Box 2713, Doha, Qatar

## ARTICLE INFO

### Article history:

Received 29 April 2013

Accepted 9 January 2014

Available online 19 February 2014

### Keywords:

Hybrid renewable energy systems

CO<sub>2</sub> emission

Optimization

PSO

Simulation

## ABSTRACT

Recently, the increasing energy demand has caused dramatic consumption of fossil fuels and unavoidable raising energy prices. Moreover, environmental effect of fossil fuel led to the need of using renewable energy (RE) to meet the rising energy demand. Unpredictability and the high cost of the renewable energy technologies are the main challenges of renewable energy usage. In this context, the integration of renewable energy sources to meet the energy demand of a given area is a promising scenario to overcome the RE challenges. In this study, a novel approach is proposed for optimal design of hybrid renewable energy systems (HRES) including various generators and storage devices. The  $\epsilon$ -constraint method has been applied to minimize simultaneously the total cost of the system, unmet load, and fuel emission. A particle swarm optimization (PSO)-simulation based approach has been used to tackle the multi-objective optimization problem. The proposed approach has been tested on a case study of an HRES system that includes wind turbine, photovoltaic (PV) panels, diesel generator, batteries, fuel cell (FC), electrolyzer and hydrogen tank. Finally, a sensitivity analysis study is performed to study the sensibility of different parameters to the developed model.

© 2014 Published by Elsevier Ltd.

## 1. Introduction

Sustainable energy (RE) systems have a pivotal role to overcome concerns over the depletion of conventional fossil fuel resources and global warming. RE systems as sustainable energy suppliers can decrease greenhouse gas (GHG) emission, transmission and transformation losses, and increase energy security. Stand alone RE sources may not meet the hourly energy demand either due to lack of the energy source level or its time variability. Hence, HRES can reduce the impact of uncertainties of the resources. In addition, the optimal design of HRES makes them cost effective, reliable and environment friendly.

Optimizing the design of an HRES is essential especially with the high present cost of an HRES and consequently adopting a sub-optimal design can significantly affect the economic performance of the HRES on the long run. Furthermore, the Kyoto protocol, adopted in 1997, obligates industrialized countries to reduce GHG

emissions. Hence, more research is required to minimize total cost and fuel emission.

Due to the complexity of optimal design of an HRES, classical optimization methods have failed to be either effective or efficient [1]. Meta-heuristics are designed to tackle complex optimization problems where other optimization methods are not able to obtain good result. Particle swarm optimization (PSO) approach is one of the meta-heuristic approaches that can be used for solving many complex problems. PSO is based on swarm intelligence. Compared with the other meta-heuristics algorithms, PSO is simple, easy to implement, and it needs fewer parameters [2].

Optimization techniques need explicit mathematical representation of the system. With complex optimization problems, it is difficult to use the mathematical model alone since the system has a high dimensional space or non-linear nature. On the other hand, simulation can be used as a tool for evaluating the performance of complex systems with almost no simplifying assumptions. However, using a simulation model alone does not obtain the optimal solution of the optimization problem. Hence, the simulation models have to be combined with an optimization search technique to deliver the optimal (or near optimal) solution. That is, developing a hybrid approach will be able to model the complex system and search for optimal solutions. This combination resulted

\* Corresponding author. Tel.: +974 44034369; fax: +974 44034301.

E-mail addresses: [tmekkawy@qu.edu.qa](mailto:tmekkawy@qu.edu.qa), [tmekkawy@hotmail.com](mailto:tmekkawy@hotmail.com) (T. Y. ELMekkawy).

## Nomenclature

$A_{PV}$	PV model area [m <sup>2</sup> ]	$P_{n-DG}$	diesel generator nominal output power [kw]
$A_{WG}$	wind turbine rotor swept area [m <sup>2</sup> ]	$P_{PV}$	PV panel capacity [kw]
$C_I$	investment cost [€/Kw]	$P_{WG}$	wind turbine capacity [kw]
$C_{O\&M}$	O& M cost [€/year]	$P_{WG,r}$	wind turbine rated power [kw]
$C_{rep}$	replacement cost [€/year]	$P_{bat}$	battery capacity [kwh]
$C_p$	power coefficient	$P_{El}$	electrolyzer capacity [kw]
CRF	capital recovery factor	$P_{tank}$	H <sub>2</sub> -tank capacity [kw]
$C_{fuel}$	fuel cost [€/year]	$P_{FC}$	fuel cell capacity [kw]
$C$	constant weighting parameter	$P_{Dis}$	diesel generator capacity [kw]
$CO_{2,emission}$	system CO <sub>2</sub> emission [kg/year]	$P_{n-FC}$	FC nominal output power [kw]
$D$	hourly energy demand [kwh]	$P_{a-FC}$	FC actual output power [kw]
$E_{PV}$	energy produced by PV panel [kwh]	$P_{id}$	best experience for particles
$E_{WG}$	energy produced by wind turbine [kwh]	PSO	particle swarm optimization
$E_{Ex}$	excess energy [kwh]	$P_{a-DG}$	diesel generator actual output power [kw]
$E_{Ex-bat}$	excess energy put into batteries [kwh]	$Q_{n-H_2}$	electrolyzer nominal hydrogen mass flow [kg/h]
$E_{Ex-El}$	excess energy put into electrolyzer [kwh]	$Q_{H_2}$	electrolyzer actual hydrogen mass flow [kg/h]
$E_{El-tank}$	energy put into H <sub>2</sub> -tank by electrolyzer [kwh]	SOC	battery state of charge [%]
$E_{tank-FC}$	energy put into fuel cell by H <sub>2</sub> -tank [kwh]	SOC <sub>min</sub>	SOC lower limit [%]
$E_{FC-load}$	energy put into load by fuel cell [kwh]	SOC <sub>max</sub>	SOC upper limit [%]
$E_{bat-load}$	energy put into load by battery [kwh]	shortage	unmet load during time step $t$ [kwh]
$E_{bat}$	power charged or discharged from battery [kwh]	SPEA	strength Pareto Evolutionary Algorithm
EF	emission factor [kg/l]	$T$	project life time [year]
EOT	equation of time [min]	$t_{zone}$	time zone difference compared to GMT [h]
$f_{FC}$	FC hydrogen consumption constant	$V$	wind speed [m/s]
$fuel_{cons}$	diesel generator fuel consumption [l/h]	$V_c$	cut-in wind speed [m/s]
$g_{id}$	global best particle	$V_r$	rated wind speed [m/s]
$H_{2,level}$	H <sub>2</sub> -tank inventory level [kg]	$V_f$	cut-off wind speed [m/s]
$H_{2,level-m}$	H <sub>2</sub> -tank inventory level upper limit [%]	$v$	particles speed vector
$H_{2,level-m}$	H <sub>2</sub> -tank inventory level lower limit [%]	$x$	particles position vector
$H_{2,cons-F}$	FC H <sub>2</sub> consumption [kg/hr]	$\eta_{FC}$	FC energy efficiency [%]
HHV <sub>H<sub>2</sub></sub>	H <sub>2</sub> higher heating value [kwh/kg]	$\eta_{El}$	electrolyzer energy efficiency [%]
HRES	hybrid renewable energy systems	$\eta_{DG}$	diesel generator energy efficiency [%]
$I_T$	total solar radiation on tilted surface [kwh/m <sup>2</sup> ]	$\eta_{H_2-tank}$	H <sub>2</sub> -tank storage efficiency
$I_{b,tilt}$	beam radiation [kwh/m <sup>2</sup> ]	$\eta_{bat}$	battery round trip efficiency [%]
$I_{d,tilt}$	sky diffuse radiation [kwh/m <sup>2</sup> ]	$\eta_{pv}$	PV model efficiency [%]
$I_{r,tilt}$	ground reflected solar radiation [kwh/m <sup>2</sup> ]	$\rho$	air density [kg/m <sup>-3</sup> ]
$I_{b,n}$	direct normal irradiance [kwh/m <sup>2</sup> ]	$\varepsilon_{LLP}$	LLP desirable level [%]
$i$	interest rate [%]	$\varepsilon_{CO_2}$	CO <sub>2</sub> emission desirable level [kg/year]
$K$	single payment worth	$\varphi$	uniform random number
LHV <sub>H<sub>2</sub></sub>	H <sub>2</sub> lower heating value [kwh/kg]	$\omega$	inertia coefficient
LHV <sub>gas oil</sub>	gas oil lower heating value [kwh/kg]	$\phi$	tilt angle from the horizontal surface [Degree]
LLP	loss of load probability [%]	$\xi$	azimuth angle [Degree]
$L$	components life time [year]	$\rho$	reflection index
LST	local standard time	$\chi$	sun zenith angel [Degree]
$L_{local}$	local longitude [Degree]	$\zeta$	plate azimuth angel [Degree]
MOP	multi objective optimization	$\delta$	solar declination angle [Degree]
$n_{max-FC}$	FC optimal operation power divide by nominal capacity [%]	$\lambda$	latitude [Degree]
		$\alpha$	solar angel [Degree]

in the development of simulation-based optimization methods which will be adopted in this paper.

In the last decade, many authors developed optimization methods to achieve several objectives for HRES: minimize emission, maximize reliability, minimize cost, etc. We divided the relevant articles into two categories, single objective (SO) and multi-objective optimization problem (MOP). Few articles used MOP for optimal design of HRES. The existing literature can further be categorized based on the considered energy resources, type of models, and solution approach. The cited articles are summarized according to these features and presented in Table 1.

Many articles used single optimization objective. Although single objective models can provide decision makers (DM) with insights into the nature of the problem, they usually cannot provide a set of alternative solutions that trade different objectives against each other. Eke et al. [3] developed a linear mathematical model to minimize total cost of an HRES. They only considered solar panels and wind turbine and used a graphical method to solve the optimization problem. Ludwig et al. [4] proposed a stochastic mixed integer programming model for a comprehensive hybrid power system design, including wind turbines, storage device, transmission network, and thermal generators. They used Benders'

**Table 1**  
Summary of the literature review.

Authors	System components								MOP based	Pareto based	Objective function	Optimization approach	Model period
	Wind turbine	PV panel	FC	Biomass	Hydro power	Geothermal	Storage	Diesel& other					
Eke et al. [3]	●	●							NO	—	Minimizes total cost	LP	1 year
Kuznia et al. [4]	●						●	●	NO	—	Minimizes total cost	SMIP	1 year
Garyfallos et al. [5]	●	●	●				●	●	NO	—	Minimizes total cost	SA	10 years
Akella et al. [6]	●	●		●	●				NO	—	Minimizes total operation cost	LP	1 year
Hanane et al. [7]	●	●	●				●		NO	—	Minimizes difference between hydrogen demand and supplied	MINLP	30 days
Cai et al. [8]	●	●			●			●	NO	—	Minimizes total cost	ISITSP	15 years
Lagorsea et al. [9]		●	●				●		NO	—	Minimizes total cost	Simulation	1 year
Orhan et al. [10]	●	●					●		NO	—	Minimizes total cost	SA	20 years
Kashefi et al. [11]	●	●	●				●		NO	—	Minimize annualized cost	PSO	20 years
Raquel and Daniel [12]	●		●				●	●	NO	—	Minimizes the LEC	LP + heuristic	1 year
Iniyar et al. [13]	●	●		●				●	NO	—	Minimize cost/efficiency ratio	LP	11 years
Juhari et al. [14]	●	●			●		●		NO	—	Minimizes cost of energy	Simulation	1 year
Katsigiannis and Georgilakis [15]	●	●					●	●	NO	—	Minimizes cost of energy	Tabu search	20 years
Budischak et al. [16]	●	●	●				●	●	NO	—	Minimizes cost of energy	Enumerative method	20 years
Elliston et al. [17]	●	●	●	●	●		●		NO	—	Minimize annualized cost	GA	1 year
Katsigiannis et al. [19]	●	●	●				●	●	Yes	Yes	Minimizes cost of energy	NSGA	1 year
Trivedi [20]	●							●	Yes	Yes	Minimizes total GHG emissions Minimizes fuel cost Minimizes SO <sub>2</sub> and NO <sub>x</sub> emission	GA	1 day
Dufo et al. [21]	●	●	●				●	●	Yes	Yes	Minimizes total cost Minimizes unmet load Minimizes fuel emission	SPEA	25 year
Abedi et al. [22]	●	●	●				●	●	Yes	Yes	Minimizes total cost Minimizes unmet load Minimizes fuel emission	DEA/Fuzzy technique	1 year
Bernal et al. [23]	●	●	●		●		●	●	NO	—	Minimizes total cost	GA	1 year
Ahmarinezhad et al. [29]	●	●	●		●		●	●	NO	—	Minimizes total cost	PSO	20 years

decomposition algorithm with Pareto-optimal cuts to solve the design problem. Garyfallos et al. [5] developed an optimization model to design a power generation systems using renewable energy sources and hydrogen storage. The model was executed in a case study that consists of photovoltaic panels, wind generators, accumulators, an electrolyzer, storage tanks, a compressor, a fuel cell and a diesel generator. They considered uncertainties to examine the effect of weather fluctuations. A stochastic simulated annealing algorithm was used to find minimum net present value of cost for ten years. Akella et al. [6] projected a linear programming model to optimize the design of an HRES which consists of micro hydro power, PV panels, wind turbine, and biomass. Hanane et al. [7] developed a mathematical programming model for a wind/PV/fuel cell/electrolyzer system to supply electricity and hydrogen to a green hydrogen refueling station network. The proposed system

was designed to meet the hydrogen needed and minimize the difference between hydrogen demands and supply. In Ref. [8] an interval-parameter superiority–inferiority-based two-stage programming (ISITSP) model has been proposed for planning renewable energy management systems. The ISITSP is the combination of interval linear programming (ILP), two-stage programming (TSP) and superiority–inferiority-based fuzzy-stochastic programming (SI-FSP). The final goal of their model is to identify the optimal capacities of facilities to minimize the sum of the relevant cost. By using Matlab/Simulink, Jeremy et al. [9] has evaluated three different HRESs based on fuel cell, PV panels and battery to simulate different configurations and investigate the operation of systems over one year. The considered criterion was minimizing the total cost. In Refs. [10–12] meta-heuristic algorithms were developed to find the optimal sizing of an HRES in order to minimize the total cost

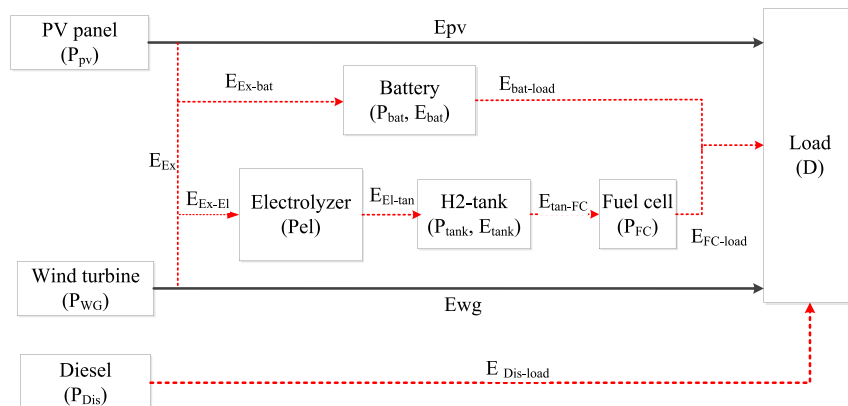


**Fig. 1.** The energy flow of the employed system.

of the system. While by using simulation approach and Tabu search algorithm in Refs. [13–15], the optimal configuration of a power generating system was presented with considering the cost of energy. Budischak et al. [16] evaluated many combinations of renewable electricity sources including inland wind, offshore wind, PV panels, and electrochemical storage incorporated into a large grid system. They used enumerative method to find the combination with minimum net present cost over 20 years. In another similar study, Ellison et al. [17] proposed a cost optimization model to find least cost options to supply the Australian National Electricity Market (NEM) using 100% renewable electricity. They considered wind, PV panels, concentrating solar thermal with storage, hydro power and biofuelled gas turbine. In their study, Genetic algorithms with integration of a simulation tool were applied to return least cost combination of renewable energy technology subject to meet NEM reliability standard. They concluded that the dominated generation mix including wind turbine, PV, CST is cheaper than a replacement fleet between 2029 and 2043 as it is projected that the carbon price will be in range of \$50–100.

In summary, although SO has been used in several HRES studies and delivers promising results, most SO methods do not address the emission affect and reliability analysis of HRES. In addition, SO lacks the capabilities providing a set of alternative solutions that compare different objectives against each other.

Multi-objective optimization problem (MOP) is another approach that has been used to design an HRES [18]. By considering conflicting objectives a set of compromised solutions, largely known as non-dominated, non-inferior or Pareto-optimal solutions can be generated [26]. We will use the following classification of search approaches which handle MOP: Pareto-based techniques and non Pareto-based techniques. The basic idea of Pareto-based techniques is that Pareto front is directly generated by using ranking and selection in the population. It requires a ranking procedure and a technique to maintain diversity in the population. Non

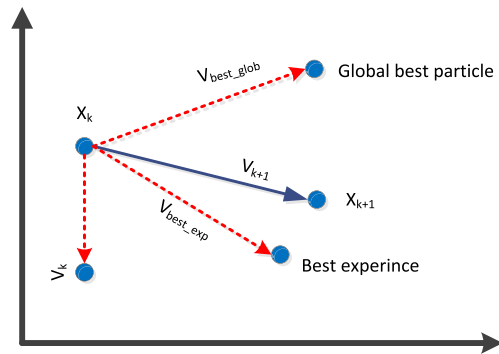


Fig. 3. Dynamic of swarms in PSO.

Pareto-based techniques are approaches that do not directly incorporate the concept of Pareto optimum [26]. Katsigiannis et al. [19] developed a multi objective optimization model to generate Pareto front to minimize the total cost of energy and total greenhouse gas emissions of an HRES during its lifetime by using non

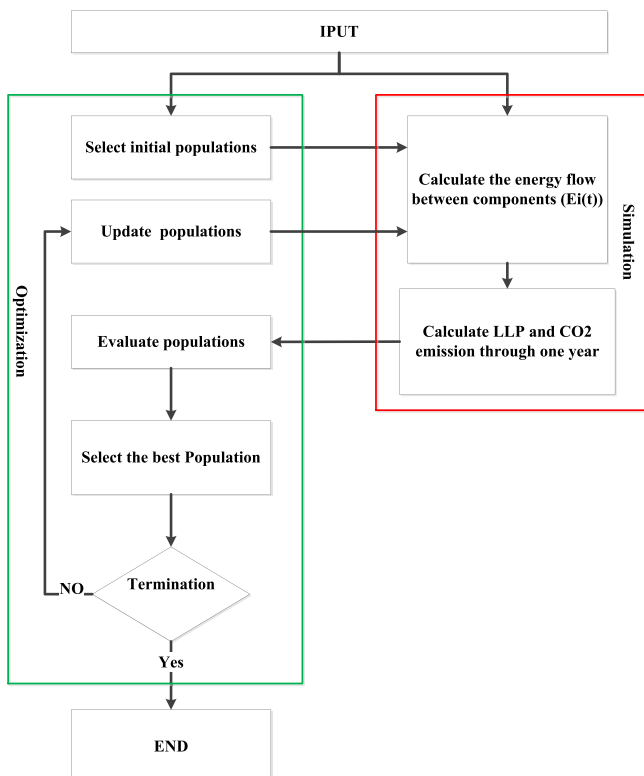


Fig. 2. PSO-simulation flowchart.

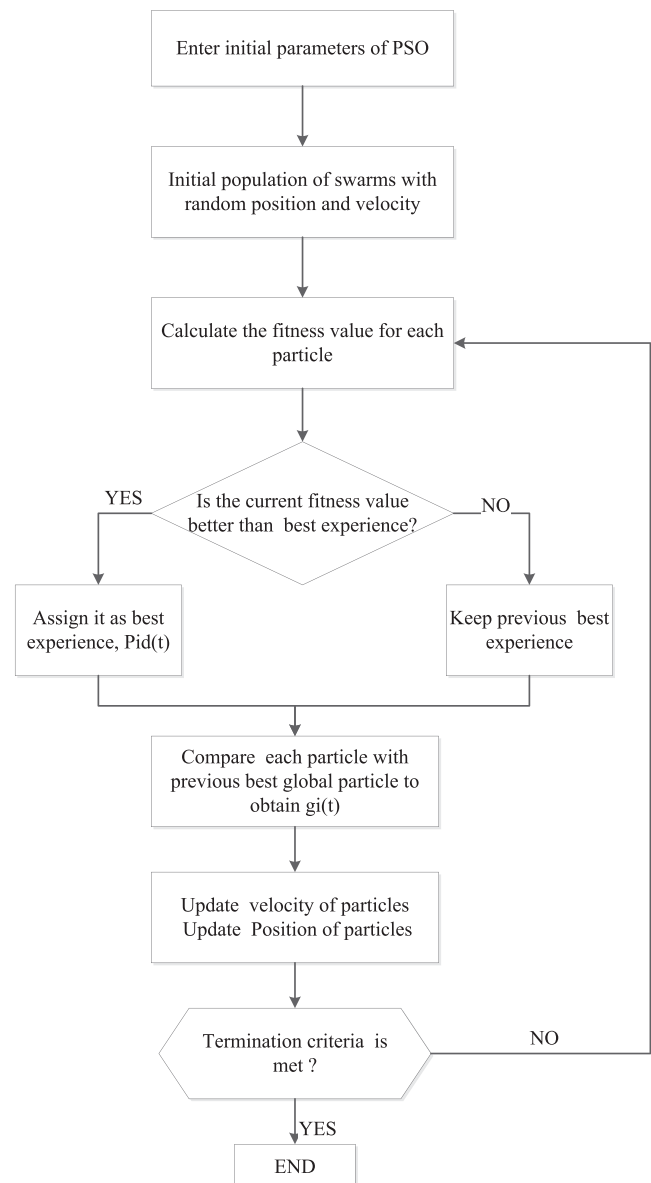


Fig. 4. PSO algorithm flowchart.

dominated sorting genetic algorithm (NSGA). In Ref. [20] multi-objective genetic algorithm (MOGA) was applied to solve a nonlinear multi objective optimization problem for scheduling a wind/diesel system, which aims to minimize fuel cost as well as SO<sub>2</sub> and NO<sub>x</sub> emission. Dufo et al. [21] applied a strength Pareto evolutionary algorithm (SPEA) to determine the optimal size and optimal power management strategy parameters for an HRES with aim of minimizing total cost, unmet load, and fuel emission simultaneously. Abedi et al. [22] presented a MOP to minimize simultaneously the total cost, pollutant emissions and unmet load. For this task, differential evolution algorithm (DEA)/fuzzy techniques have been used to find the best combination of components and control strategies for the HRES.

In brief, although few articles have applied MOP to design an HRES, they are usually using MOEA Pareto-based techniques which require expensive ranking and pairwise comparison operations [30].

In this paper, a novel approach is proposed for optimal design of HRES including various generators and storage devices. The  $\epsilon$ -constraint method which is a non Pareto-based search technique has been applied to minimize simultaneously the total cost of the system, unmet load, and fuel emission. The idea of this approach is to minimize the total cost while CO<sub>2</sub> emission and unmet load are considered as constraint bound by permissible levels. By varying these levels, the non-inferior solutions can be obtained. PSO-simulation based technique has been used to handle the developed multi-objective optimization problem. The attractive features of this proposed approach are its simplicity [26,30], or it needs relatively less computational effort since excessive operations of ranking and pairwise comparison that are required by Pareto-based techniques are eliminated [30]. Moreover, the model is flexible to consider simultaneously more renewable sources and storage devices.

The rest of the paper is organized as following. First the problem description and the proposed approach are given in Sections 2, and 3 respectively. The simulation module of the proposed approach and the mathematical models of system's components are described in section 4. Section 5 is devoted to explaining the optimization module and the proposed PSO algorithm. The results of optimizing a case study along with sensitivity analysis result are exhibited in Section 6. Finally, conclusion and future research are given in Section 7.

## 2. Problem description

The considered hybrid renewable energy system in this study is adopted from Refs. [21,23]. The system includes PV panels, wind turbine, diesel generator, and two storage systems. Battery and electrolyzer/hydrogen tank/FC are the storage devices. The energy flow of the employed system is shown in Fig. 1. The PV panels and wind turbine produce electricity from solar and wind energy to meet the energy requirement of a specific area. When the energy produced is more than the needed load, the excess energy is stored in the storage systems. A share of excess energy is put into batteries and the reminding energy is put into the electrolyzer and converted to hydrogen. The hydrogen produced by the electrolyzer is stored in the H<sub>2</sub>-tank. When the energy produced by PV panels and wind turbines cannot meet the load, the batteries and fuel cell can provide power to meet the load based on the state of charge of batteries and H<sub>2</sub> level of the tank. When the batteries and H<sub>2</sub>-tank are not able to meet the deficit energy, the diesel generator is used as an emergency power-supply.

## 3. Proposed approach

This study attempts to emphasize optimization of a HRES design by using a PSO-simulation based approach. Simulation can be used

as an effective evaluation tool whenever mathematical models are not applicable due to system complexity or existing uncertainties. The main advantage of using simulation modeling is the fact that all system's details and uncertainties can be accommodated accurately compared to other modeling methodologies. However, simulation inherently cannot be used as a stand-alone tool to deliver the optimal design of the system. On the other hand, optimization techniques need explicit mathematical representation of the system. In complex systems, it is difficult to develop the mathematical model since the system has a high dimensional space or non-linear nature. Therefore, combining simulation model with an optimization method allows overcoming their shortcomings. That is, the hybrid approach is able to model the complex features of the system as well as obtaining the optimal solution in reasonable time. In this paper, to find the optimal (or near optimal) design of the HRES, we have proposed the PSO-simulation based approach as outlined in Fig. 2 and Fig. 4. The proposed approach can change and evolve to incorporate additional elements of the HRES.

The decision variables, fitness and constraints are defined in the PSO algorithm. Design variables that are the capacity of the components are defined in a vector named particle. In other word, each particle represents a certain configuration of the HRES. Total cost which is a function of design variables is considered as the fitness of particles for particles evaluation. Moreover, each particle generated randomly should meet the constraints of the model which will be presented in Section 5.2. After initializing a population of particles, each particle is sent to the simulation model for checking its feasibility. The simulation model is run for one year to evaluate the performance of each particle. The simulation model calculates the yearly unmet load and CO<sub>2</sub> emission for the HRES using the equations which are presented in section 4. In the next step, values of unmet load and CO<sub>2</sub> emission are sent to the optimization algorithm to check if the particle meets the desirable level of unmet load and CO<sub>2</sub> emission. If the particle did not meet the constraints, it is modified and sent back to simulation. After initializing feasible particles, they are evaluated in the PSO algorithms based on their fitness. Stopping criterion is checked, if it is not met, each particle is updated for next generation in the framework of the PSO algorithm, Section 5.3 and Fig. 4. After updating, the particles are sent back to simulation model to review their feasibility again and the simulation result is sent to optimization algorithm for evaluation. This cycle is terminated if the stopping criterion is met. After terminating the cycle, the best of all considered solutions will be returned.

## 4. Simulation module

As mentioned in the previous section, the simulation model is run for checking the feasibility of a particle that represents a certain configuration of the HRES for one year. The simulation output is the yearly unmet load and CO<sub>2</sub> emission for that HRES configuration. The considered HRES in this paper is depicted in Fig. 1. The HRES includes seven main components comprising PV/wind turbine/diesel/batteries/FC/electrolyzer/H<sub>2</sub>-tank. The simulation model is based on the hourly time interval analysis of electricity demand, wind speed, and solar irradiation. The wind model converts the hourly wind velocity to the energy output. Similarly, the PV model converts the total radiation on the horizontal surface to energy output. The diesel model uses the fuel consumption curve data, for a given choice of diesel generator, to calculate output. The electrolyzer model calculates the hydrogen production by using coefficients of its electrical consumption curve. FC model uses the hydrogen consumption curve to calculate the hydrogen consumed from the hydrogen tank. The battery and hydrogen tank models use the excess energy and deficit energy to update the battery state of charge and hydrogen level,



respectively. The components mathematical models which are used in the simulation are summarized below.

- Wind turbine: Essentially in wind turbines, wind power generation is produced from conversion of wind kinetic energy into electrical energy. Energy resulted from a wind turbine is calculated by Eq. (1) [10,31].

$$E_{WG}(t) = \begin{cases} 0 & v < V_c \\ \frac{1}{2} C_p \rho A_{WG} v^3(t) \Delta t & V_c < v < V_r \\ P_{WG,r} & V_r < v < V_f \\ 0 & v > V_f \end{cases} \quad (1)$$

Wind speed for each time period  $V(t)$  is as an input of the model.  $C_p$  is the coefficient of performance and it is defined as the ratio of the power output of a wind generator divided by maximum power. It is a characteristic of wind turbines obtained from the manufacture firm. The rotor swept area is named  $A_{WG}$  and the air density is equal to  $\rho$ .  $V_c$  is cut-in wind velocity which is considered 4 (m/s).  $V_r$  is rated wind velocity is set as 14 (m/s) and  $V_f$  is cut-off wind speed considered 20 (m/s) [21].  $P_{WG,r}$  is the wind turbine rated power [21].

- PV panel: Solar or photovoltaic cells are electronic devices that convert the solar energy of sun light into electricity. Produced energy by PV panels is calculated by Eq. (2) [10].

$$E_{PV}(t) = (\eta_{pv} A_{pv}) I_T(t) \quad (2)$$

where,  $I_T(t)$  is hourly total solar radiation on tilted surface,  $\eta_{pv}$  is PV modules efficiency and  $A_{pv}$  stands for the PV panel area(m<sup>2</sup>). In this study,  $\eta_{pv}$  is assumed to be constant and is equal to 7%. This value covers power losses in PV panel due to temperature change, shadows, dirt, losses in inverter, etc. Solar radiation on a tilted surface having a tilt angle of  $\phi$  from the horizontal surface and an azimuth angle of  $\xi$  is the sum of components consisting of beam ( $I_{b,tilt}$ ), sky diffuse ( $I_{d,tilt}$ ) and ground reflected solar radiation ( $I_{r,tilt}$ ) [32]:

$$I_T = I_{b,tilt} + I_{d,tilt} + I_{r,tilt} \quad (3)$$

$$I_T = I_{tilt} = I_{b,n} \left[ \cos(\theta) + C \cos^2\left(\frac{\phi}{2}\right) + \rho(\cos\chi + C) \sin^2\left(\frac{\phi}{2}\right) \right] \quad (4)$$

where,  $I_{b,n}$  is direct normal irradiance on a surface perpendicular to the sun's rays, " $\theta$ " is the angle between the tilted surface and the solar rays which is calculated by Eq. (5),  $C$  is diffuse portion constant for calculation of diffuse radiation,  $\rho$  is the reflection index, and  $\chi$  is the zenith angel.

$$\cos(\theta) = [\cos \phi \cos \chi + \sin \phi \sin \chi \cos(\xi - \zeta)] \quad (5)$$

$\xi$  and  $\zeta$  are stand for sun azimuth and plate azimuth angel, respectively. The Eq. (6) and Eq. (7) are used to calculate the sun zenith and azimuth angel [32]:

$$\cos \chi = \sin \delta \sin \lambda + \cos \delta \cos \lambda \cos \alpha \quad (6)$$

$$\tan \xi = \frac{\sin \alpha}{\sin \lambda \cos \alpha - \cos \lambda \tan \delta} \quad (7)$$

where,  $\delta$  is solar declination angle and is calculated by Eq. (8),  $\lambda$  is latitude per degree and  $\alpha$  is solar angel which is determined by using Eqs. (9)–(12) [32].

$$\delta = 23.44 \sin \left[ 360 \left( \frac{d - 80}{365.25} \right) \right] \quad (8)$$

$$\alpha = \frac{360}{24} (t - 12) \quad (9)$$

$$t = LST + EOT - 4L_{local} + 60t_{zone} \quad (10)$$

$$B = 360(n - 81)/364 \quad (11)$$

$$EOT (\text{minutes}) = -(9.87 \sin 2B - 7.53 \cos B - 1.5 \sin B) \quad (12)$$

where,  $d$  is number of day when January 1st is equal to one.  $t$  is solar time and identified by Eq. (10) [32].  $LST$  is local standard time or real time;  $EOT$  is equation of time to account for irregularity of the earth speed around the sun (minutes);  $L_{local}$  is local longitude (degrees East > 0 and West < 0) and  $t_{zone}$  is the time zone difference compared to GMT (East > 0 and West < 0) [32].

- Electrolyzer: In electrolyzer, hydrogen and oxygen gases are generated from water by using electrical energy. In this study, the electrolyzer electrical consumption ( $E_{EL}$ ) is modeled as a function of nominal hydrogen mass flow ( $Q_{n-H_2}$ ) and actual hydrogen mass flow ( $Q_{H_2}$ ) as given in Ref. [21]:

$$E_{EL} = \alpha_E Q_{n-H_2} + \beta_E Q_{H_2} \quad (13)$$

where,  $\alpha_E$ ,  $\beta_E$  are the coefficients of electrical consumption curve per hydrogen mass flow. The electrolyzer efficiency is defined as the heating value of produced hydrogen divide by electrical consumption, Eq. (14) [21].

$$\eta_{EI} = \frac{Q_{H_2} \times HHV_{H_2}}{E_{EL}} \quad (14)$$

In this study,  $HHV_{H_2}$  is equal to 39.4 kwh/kg,  $\alpha_E = 20$  kwh/kg, and  $\beta_E = 40$  kwh/kg [21].

- Fuel cell: Fuel cells which convert the chemical energy of hydrogen and oxidant to electrical energy are selected as a backup generator. The output power of a fuel cell can be expressed as a function of the hydrogen consumption of fuel cell ( $H_{2,cons-FC}$ ) Eq. (15) [21].

$$\begin{cases} H_{2,cons-FC} = \alpha_{FC} P_{n-FC} + \beta_{FC} P_{a-FC} & \text{if } \frac{P_{a-FC}}{P_{n-FC}} \leq n_{max-FC} \\ H_{2,cons-FC} = \alpha_{FC} P_{n-FC} + \beta_{FC} P_{a-FC} (1 + f_{FC} \left( \frac{P_{a-FC}}{P_{n-FC}} - n_{max-FC} \right)) & \text{if } \frac{P_{a-FC}}{P_{n-FC}} \geq n_{max-FC} \end{cases} \quad (15)$$

where  $\alpha_{FC}$ ,  $\beta_{FC}$  are the coefficients of hydrogen consumption curve, which are defined by users.  $P_{n-FC}(kW)$ ,  $P_{a-FC}(kW)$  are the nominal output power and actual power of fuel cell.  $n_{max-FC}$  in % of  $P_{n-FC}$  is the power that FC has maximum efficiency and  $f_{FC}$  is a constant. In this study  $\alpha_{FC} = 0.004 \text{ kg/kWh}$ ,  $\beta_{FC} = 0.05 \text{ kg/kWh}$ ,  $f_{FC} = 1$ .  $\eta_{FC}$  is the energy efficiency and it is defined by Eq. (16) [21,22,24].

$$\eta_{FC} = \frac{P_{a-FC}}{H_{2\text{cons-FC}} \times \text{LHV}_{H_2}} \quad (16)$$

- Diesel generator: Diesel generator sets are used as emergency power-supply. In this study, the fuel consumption of a diesel generator depends on the generator size and the load at which the generator is operating. The fuel consumption of a diesel generator is approximated by Eq. (17) [21].

$$\text{fuel}_{\text{cons}} = \alpha_{DG} P_{n-DG} + \beta_{DG} P_{a-DG} \quad (17)$$

where,  $\alpha_{DG}$  and  $\beta_{DG}$  are the coefficients of fuel consumption curve,  $P_{n-DG}$  and  $P_{a-DG}$  are nominal capacity and power output of the diesel generator, respectively. In this study,  $\alpha_{DG} = 0.081451 \text{ l/kWh}$  and  $\beta_{DG} = 0.2461 \text{ l/kWh}$ . The diesel generator efficiency,  $\eta_{DG}$ , is defined as power output divide by heating value of fuel consumption [21].

$$\eta_{DG} = \frac{P_{a-DG}}{\text{fuel}_{\text{cons}} \times \text{LHV}_{\text{Gas oil}}} \quad (18)$$

where,  $\text{LHV}_{\text{Gas oil}}$  is the lower heating value of gas oil and is equal to 10–11.6 kWh/lit [21].

- Battery: The state of charge of battery at any time step is calculated by using following equation [22]:

$$\text{SOC}(t) = \text{SOC}(t-1) \pm \frac{E_{\text{bat}}(t) \eta_{\text{bat}}}{P_{\text{bat}}} \cdot 100 \quad (19)$$

Positive sign is for charging modes and negative one is for discharging. Where,  $\text{SOC}(t)$  and  $\text{SOC}(t-1)$  are the state of charge of battery in time step  $t$  and  $t-1$ ,  $\eta_{\text{bat}}$  is the battery round trip efficiency,  $E_{\text{bat}}(t)$  is power charged or discharged from battery during time step  $t$  and  $P_{\text{bat}}$  (kWh) is nominal capacity of battery. The battery can supply energy to demand until the lower limit of  $\text{SOC}_{\min}$ . Moreover, the battery can be charged until  $\text{SOC}_{\max}$  is reached. In this study,  $\eta_{\text{bat}}$  is considered 80% in charging state and 100% in discharging state,  $\text{SOC}_{\min} = 30\%$  and  $\text{SOC}_{\max} = 100\%$  [22].

- Hydrogen tank: Hydrogen level of  $H_2$ -tank at time step  $t$  depends on hydrogen level at time  $t-1$  ( $H_2(t-1)$ ), output hydrogen mass flow of electrolyzer at time step  $t$  ( $Q_{H_2}$ ), and hydrogen consumption of FC at time  $t$ , ( $H_{2\text{cons-FC}}(t)$ ), i.e. [11]:

$$H_{2\text{level}}(t) = H_{2\text{level}}(t-1) + Q_{H_2}(t) - \frac{H_{2\text{cons-FC}}(t)}{\eta_{H_2\text{-tank}}} \quad (20)$$

where,  $\eta_{H_2\text{-tank}}$  represents the storage efficiency which is indicated losses associated with leakage and pumping. In this study,  $\eta_{H_2\text{-tank}}$  is assumed 95%. Furthermore, there is upper and lower limit for hydrogen level. The upper limit is the nominal capacity of tank and lower limit is considered 5% of the rated capacity

- Dispatch strategy: When the produced energy by wind turbines and PV panels is more than the load, the excess energy is stored in the storage systems. First, the excess energy put into batteries until the  $\text{SOC}_{\max}$  is reached, if there is excess energy yet, the excess energy is converted to  $H_2$  in the electrolyzer and stored in the  $H_2$ -

tank. In other words, the batteries have the highest priority for charging. If the produced renewable energy is less than the load, the batteries and fuel cell are respectively used to provide the difference in power. If the power shortage exceeds the stored power in both storage devices, the diesel generator is used to meet the load. If this shortage goes beyond generator rated capacity, the shortage is considered as unmet load. After discharging the storage level of batteries and  $H_2$ -tank are updated, Eq. (19) and Eq. (20).

- LLP and  $\text{CO}_2$  emission: As the most of the exhaust gases of the diesel generator is  $\text{CO}_2$ , in this study the number of kg produced  $\text{CO}_2$  by diesel generator is considered to represent the pollutant emission. For each time period during one year the shortage of energy, loss of load probability (LLP) and  $\text{CO}_2$  emission calculated by using Eq. (21)–(22) [21,22].

$$\text{LLP} = \frac{\sum_{t=1}^{8760} \text{shortage}(t)}{\sum_{t=1}^{8760} D(t)} \quad (21)$$

$$\text{CO}_{2\text{emission}} = \sum_{t=1}^{8760} \text{fuel}_{\text{cons}}(t) \times \text{EF} \quad (22)$$

where,  $D(t)$  is electricity demand, and  $\text{shortage}(t)$  is unmet load during time period  $t$ , EF is the emission factor for diesel generator, which depends on type of fuel and diesel engine characteristics. Here this is considered as 2.4–2.8 kg/lit rang [21].

## 5. Optimization module

### 5.1. The $\epsilon$ -constraint method

The  $\epsilon$ -constraint method is a simple MOP technique that can be used where one objective is chosen to be optimized and the remaining objectives are considered as constraints bound by given target levels ( $\epsilon_i$ ) [25]. By varying these levels, the non-inferior solutions of introduced problem can be obtained. Consider the following MOP:

$$\text{Min } \{f_1(x), f_2(x), \dots, f_k(x)\}$$

where,  $x$  is the decision vector,  $f_i$  ( $i = 1, 2, \dots, k$ ) are objective functions. A solution  $x^*$  is said to be non-inferior if there exists no other feasible solution  $x$  such that  $f_i(x) \leq f_i(x^*)$  for all  $i = 1, 2, \dots, k$ , and at least one inequality is strict.

In  $\epsilon$ -constraint method, if  $f_j(x)$ ,  $j \in \{1, \dots, k\}$  is the objective function chosen to be optimized, and  $f_i(x)$  is objective considered as the constraint, we have the following problem [25,26]:

$$\text{Min } f_j(x) \quad j \in \{1, \dots, k\}$$

Subject to

$$f_i(x) \leq \epsilon_i \quad \forall i \in \{1, \dots, k\}, i \neq j, x \in S$$

where,  $S$  is the feasible solution space,  $k$  is number of objective functions, and  $\epsilon_i$  is assumed values of the objective function that must not be exceeded.

In this paper, three objective functions are considered. These three objective functions are minimizing the total cost of the system, the total  $\text{CO}_2$  emissions produced by diesel generators, and LLP. The overall cost of the system includes the investment cost, operation and maintenance cost, replacement cost, and fuel cost of diesel generators during the lifespan of the system. LLP represents the energy deficit, which is the ratio of the unmet load to the total load. In the proposed  $\epsilon$ -constraint approach, the total cost is chosen

as the objective function to optimize and total CO<sub>2</sub> emission and LLP incorporate as inequality constraints in the forms:  $CO_2_{\text{emission}} \leq \epsilon_{CO_2}$  and  $LLP \leq \epsilon_{LLP}$ . Hence in this study,  $k = 3$ ,  $\epsilon_{CO_2}$  and  $\epsilon_{LLP}$  are chosen by DMs as the desirable values.

## 5.2. Objective functions and constraints

AS it was mentioned earlier, the total cost over the lifetime of the HRES is considered as objective function and CO<sub>2</sub> emission and LLP during one year are considered as the constraint bounds. The life time of the system is considered 25 years same as life of the PV panels, which are the elements that have a longer lifespan [21]. Decision variables of the model are summarized in the following vector:

$$P = [P_{PV}, P_{WG}, P_{bat}, P_{EL}, P_{tank}, P_{FC}, P_{Dis}]$$

where,  $P_{WG}$  is the capacity of the wind turbine (kw),  $P_{PV}$  is the capacity of PV panels (kw),  $P_{bat}$  is the capacity of batteries (kwh),  $P_{FC}$  is the capacity of fuel cell (kw),  $P_{EL}$  is the capacity of electrolyzer (kw),  $P_{tank}$  is the capacity of H<sub>2</sub>-tank (kwh), and  $P_{Dis}$  is the capacity of diesel generator (kw). The system costs consist of investment cost, operation and maintenance cost, fuel cost, and replacement cost over the project life time Eq. (23).

$$\text{cost} = \sum_j \left[ C_{Ij} + C_{O\&Mj} \times \frac{1}{CRF(i, T)} + C_{repj} \times K_j \right] \times P_j + C_{fuel} \times \text{fuel}_{\text{cons, yr}} \times \frac{1}{CRF(i, T)} \quad (23)$$

where,  $j$  is component indicator,  $C_{Ij}$  is the capital cost per unit for the component  $j$  (€/unit),  $C_{O\&Mj}$  is the operation and maintenance cost per unit for the component  $j$  (€/unit),  $C_{fuel}$  is the fuel cost (€/lit),  $C_{repj}$  is the cost of each replacement per unit for the component  $j$  (€/unit), and  $P_j \in \{P_{PV}, P_{WG}, P_{bat}, P_{EL}, P_{tank}, P_{FC}, P_{Dis}\}$ ,  $\text{fuel}_{\text{cons, yr}}$  is the annual fuel consumption (lit/year).  $K_j$  and CRF are single payment present worth and capital recovery factor, respectively, which are calculated using the following equations, Eq. (24–26) [11,21,22].

$$K_j = \sum_{n=1}^Y \frac{1}{(1+i)^{L \times n}} \quad (24)$$

$$\begin{cases} Y = \left\lceil \frac{T}{L} \right\rceil - 1 & T\%L = 0 \\ Y = \left\lceil \frac{T}{L} \right\rceil & T\%L \neq 0 \end{cases} \quad (25)$$

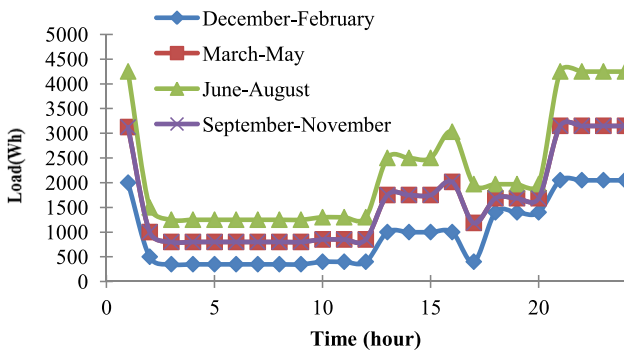


Fig. 5. Daily load profile in the various seasons.

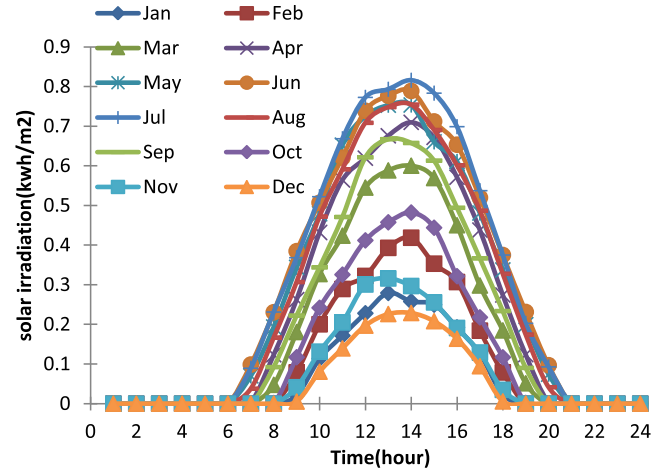


Fig. 6. Hourly solar irradiation during one year.

$$CRF = \frac{i(1+i)^T}{(1+i)^T - 1} \quad (26)$$

where,  $i$  is the real interest rate,  $L$  and  $Y$  are life time and number of replacement of the component  $j$ , respectively, and  $T$  is the project life time which is considered 25 years in this study.

The problem constraints that should be met are: the LLP of the system should be less than allowable LLP reliability index Eq. (27). The CO<sub>2</sub> emission should be less than allowable emission level Eq. (28). In addition, energy and storage level of components are subjected to some other feasible operation constraints. The energy flow (energy produced by or entered to each component) in every time ( $E_j(t)$ ) should be less than the capacity of the component Eq. (29). Where,  $\Delta t$  is the time interval that is 1 h. As mentioned in Section 4, the batteries can supply energy to load until the lower limit of SOC<sub>min</sub>, and can be charged until SOC<sub>max</sub> is reached Eq. (30). Furthermore, there is upper and lower limit for hydrogen level which is presented in Section 4, Eq. (31). Finally, there are non-negativity constraints for decision variables and energy flow as well as upper limit for decision variables Eq. (32), (33).

$$LLP \leq \epsilon_{LLP} \quad (27)$$

$$CO_2_{\text{emission}} \leq \epsilon_{CO_2} \quad (28)$$

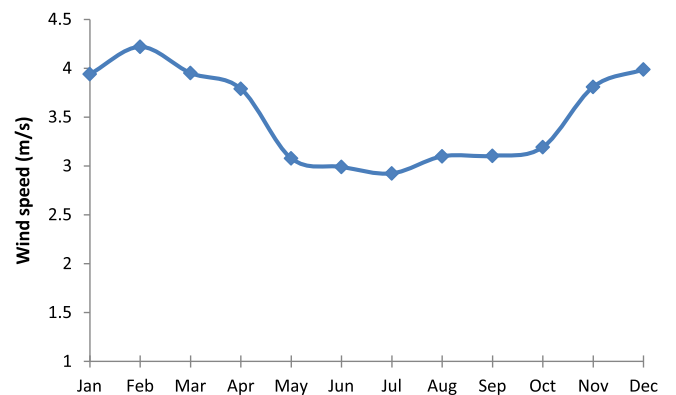


Fig. 7. Average monthly wind speed at 10 m height during one year.



**Table 2**  
Characteristics of components.

Components	PV panel	Wind turbine	Fuel cell	Electrolyzer	H <sub>2</sub> tank	Battery	Diesel generator
Life time	25 yr	20 yr	15,000 h	10 yr	20 yr	5 yr	7000 h

$$E_j(t) \leq P_j \times \Delta t \quad (29)$$

$$\text{SOC}_{\min} \leq \text{SOC}(t) \leq \text{SOC}_{\max} \quad (30)$$

$$H_{2\text{level-min}} \leq H_{2\text{level}}(t) \leq H_{2\text{level-max}} \quad (31)$$

$$0 \leq P_j \leq P_{\max,j} \quad (32)$$

$$E_j(t) \geq 0 \quad (33)$$

### 5.3. Particle swarm optimization algorithm

PSO, a meta-heuristic optimization technique, was firstly developed by Kennedy and Eberhart in 1995. PSO algorithm is able to solve continuous problems as well as binary or discrete problems. It is a “multi agent parallel search technique” that is inspired by the social behavior of “bird flocking” or “fish schooling” [27]. In PSO, a set of particles or swarms which are described by their position and velocity vector fly through the search space by following the current optimum particle. Particles motions are defined by a vector, which defines the velocity of the swarm in the each direction. The best solution for each particle obtained so far is stored in the particle memory and named particle experience. In addition,

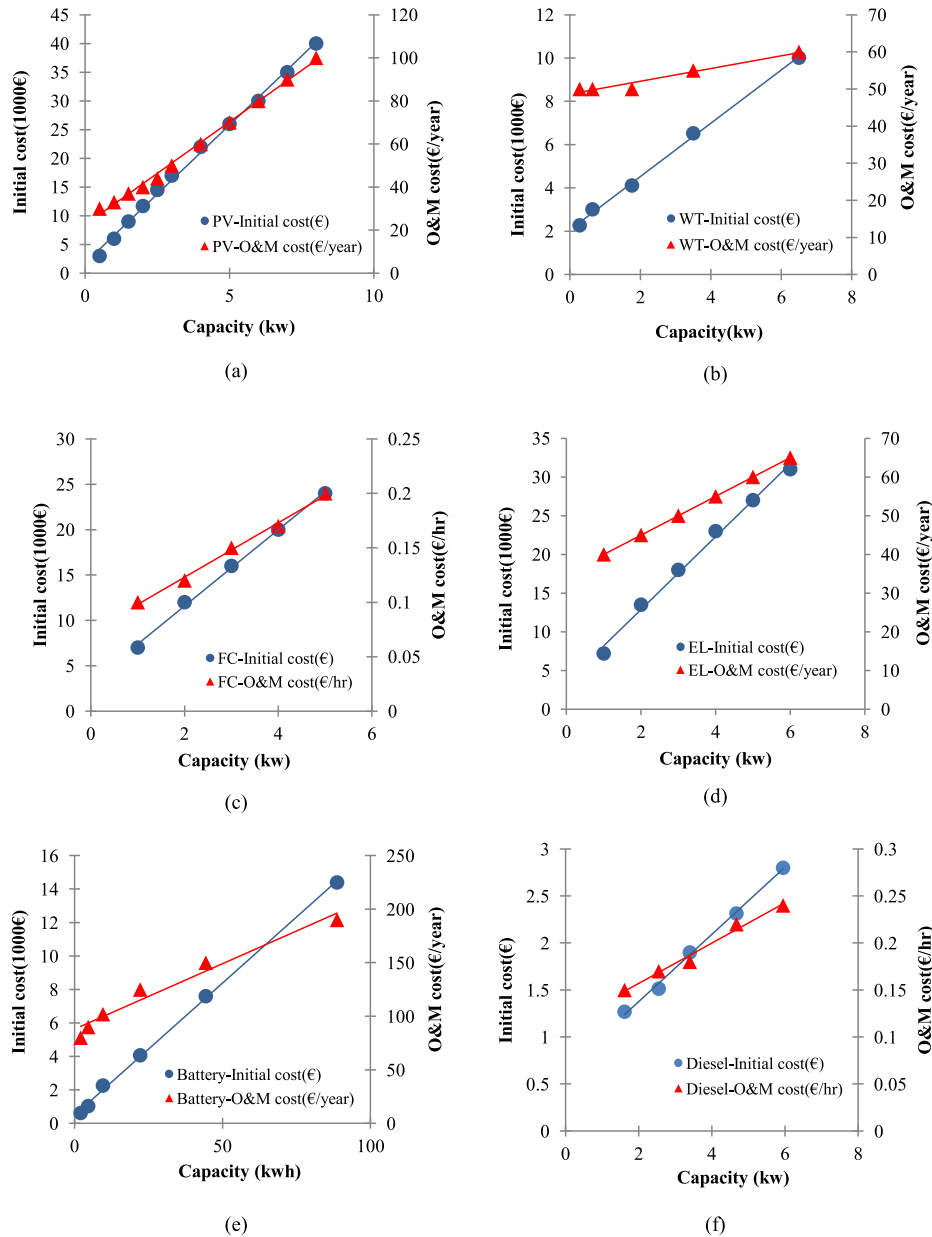


**Fig. 8.** Components initial cost and operation and maintenance (O&M) cost: (a) PV panel costs, (b) Wind Turbine cost, (c) fuel cell costs, (d) Electrolyzer costs, (e) Battery costs, (f) Diesel generator costs.

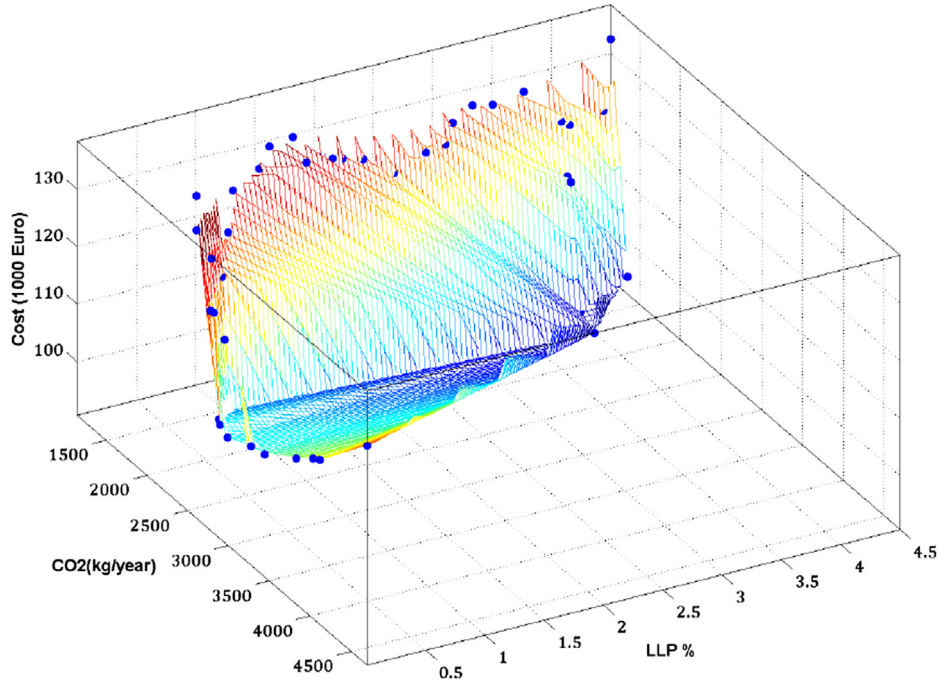


Fig. 9. 3D set of non-inferior solutions obtained by the  $\epsilon$ -constraint method.

the best obtained solution among all particles so far is named the best global particle. The velocity and position for each swarm is updated according to its experience and the best global particle. The experience sharing of each particle with other swarms is the most important reason behind PSO success, and it leads the particle move to better region [27].

First a random population of swarms is generated with random position vectors ( $\vec{x}$ ) and velocity vectors ( $\vec{v}$ ). The fitness value of each particle is calculated to evaluate the current position of particles and compare it with its best experience and other swarms fitness value. If the current position of the particle is better than best historically obtained one, the experience of the particle is adjusted. Moreover, the velocity of a particle is adjusted according to global best particle and its best own experience. In fact, particles move toward the best global particle in the each iteration. Finally, the best global particle is updated, Fig. 3.

As mentioned earlier, each particle has two state variables, its current position  $\vec{x}_i(t)$  and its velocity  $\vec{v}_i(t)$ . The best experience for each particle is stored in the particle memory  $\vec{p}_i(t)$  while  $\vec{g}(t)$  denotes the best global particle among the population. In each iteration, the  $d$ th dimension of the position and velocity of the particles are updated toward the best experience and the best global particle by applying recursive Eq. (34), (35) [28].

$$v_{id}(t+1) = \omega \cdot v_{id}(t) + C_1 \cdot \varphi_1 \cdot (P_{id}(t) - x_{id}(t)) + C_2 \cdot \varphi_2 \cdot (g_{id}(t) - x_{id}(t)) \quad (34)$$

$$x_{id}(t+1) = x_{id}(t) + v_{id}(t+1) \quad (35)$$

The velocity updating equation has three main terms: The first term ( $v_{id}(t)$ ) stands for the inertia velocity and  $\omega$  is called the inertia coefficient. This term ensures that the velocity of each particle is not changed abruptly, but rather the previous velocity of the particle is taken into consideration. That is why the particles generally tend to continue in the same direction they have been flying. The parameters  $c_1$  and  $c_2$  are positive weighting constants, and denoted as the “self-confidence” and “swarm confidence”, respectively. They control the movement of each particle towards its individual versus global best position. The parameters  $\varphi_1$  and  $\varphi_2$  are two uniform random numbers with interval (0 1) [28]. The first iteration is terminated by adjusting the velocities and positions for the next time step  $t+1$ . Consistently, this process is executed until a certain stopping criterion is met. The stopping criterion can be the

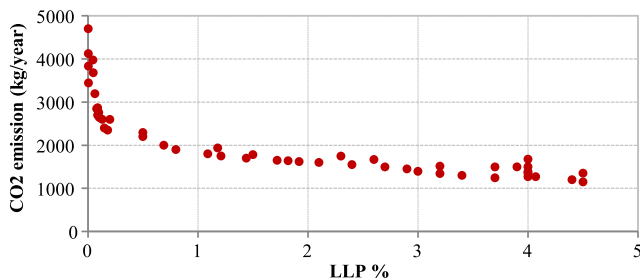


Fig. 10. 2D set of non-inferior solutions. CO<sub>2</sub> emission vs. LLP.

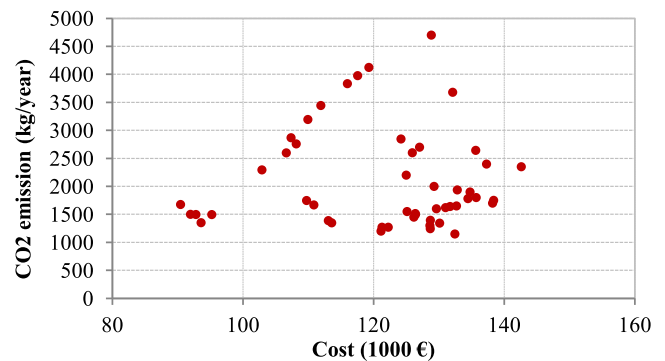


Fig. 11. 2D set of non-inferior solutions. CO<sub>2</sub> emission vs. cost.

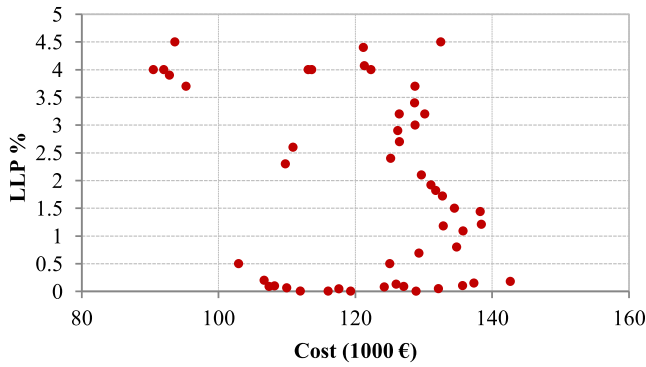


Fig. 12. 2D set of non-inferior solutions. LLP emission vs. cost.

maximum number of time steps, improvement of the best objective function value, or average value computed from the whole population objective function value. Fig. 4 shows PSO algorithm that is explained above.

The main parameters of PSO algorithm are  $\omega$ ,  $c_1$ ,  $c_2$  and the swarm size. These parameters are exogenous which are initialized by users before an execution. An optimal setting of the parameters depends on the problem at hand. According to literature a suitable interval for setting PSO parameters are suggested as following:

- **Inertia weight  $\omega$ :** the high settings in the range [0.5, 1] and near 1 facilitates global search [28].
- **Swarm size:** depending on problem search space, the number of particles can be in the range (20–60) [28].
- **Acceleration coefficients:** Usually an equal value of  $c_1$  and  $c_2$  is used within the range [0, 4] [28].

The above mentioned intervals are used in an exhaustive study to obtain the best values of these parameters. That is, the PSO parameters were changed in the intervals and the performance of PSO was monitored. The result of the study shows that the appropriate value for the parameters are at population size = 60,  $c_1 = 0.25$ ,  $c_2 = 1.75$ , and  $\omega = 1$ . The maximum number of iteration is set to 1000.

## 6. Results

The proposed approach was coded in C++ programming environment in a 2.4 GHz core 2 processor. By implementing the

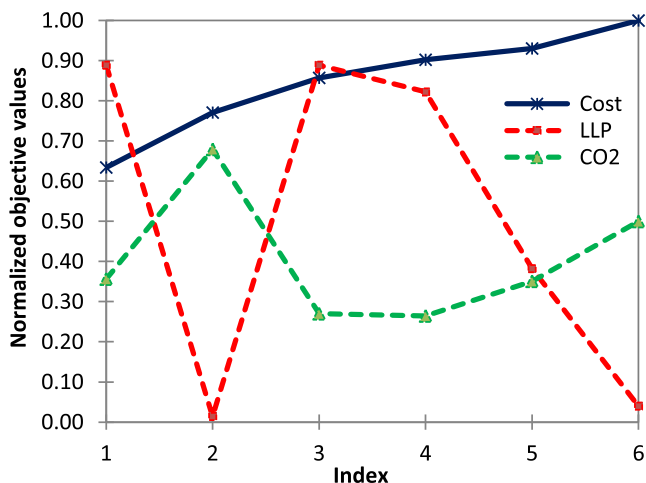


Fig. 13. Pruned solutions when cost objective function is preferred.

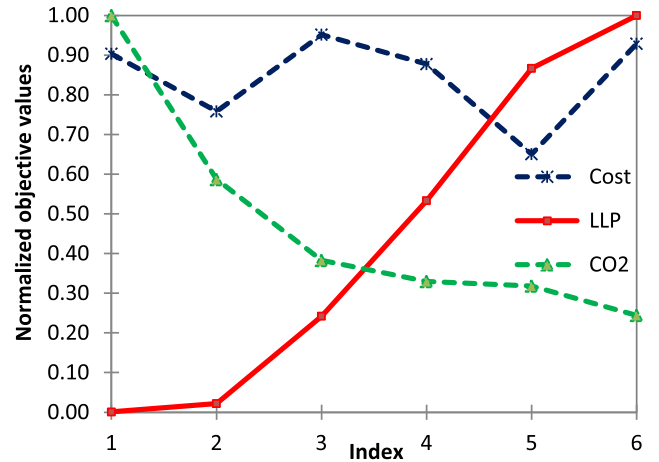


Fig. 14. Pruned solutions when LLP objective function is preferred.

approach, a stand-alone hybrid system including PV panels/wind turbine/batteries/fuel cell/H<sub>2</sub> tank/electrolyzer/diesel generator system has been designed to supply power for a remote area at Zaragoza (latitude 41.65°), Spain. Daily load variation in the various seasons is shown in Fig. 5. The time step is considered 1 h and during this time step the wind energy, solar energy and load are assumed to be constant [21].

The daily solar irradiation on the horizontal surface and wind speed data at 10 m height are plotted in Figs. 6 and 7 which are obtained by the average of last 10 years data.

The initial cost, operation cost, and characteristics of components vary with their size and model. In this study, the initial cost, maintenance cost, and characteristics of components are presented in Table 2 and Fig. 8 [11,21,22,29].

The initial cost of H<sub>2</sub>-tank is assumed 1000 €/kg, its operation and maintenance cost is 50 €/year. The considered fuel is gas oil and its price is 1.2 €/lit with 10% inflation rate [21].

The set of non-inferior solutions obtained by the  $\epsilon$ -constraint method is shown in Figs. 9–12. In these figures, there are 50 solutions in the non-inferior set which demonstrate the minimum total cost of system for different LLP and CO<sub>2</sub> emission. The range in the objective space is obtained by varying  $\epsilon_{LLP}$  and  $\epsilon_{CO_2}$ . It can be seen in these figures that CO<sub>2</sub> emission of the system decrease significantly as the LLP increase to about 0.15%. Increasing the LLP of the system from 0.15% to 4.5% decreases the CO<sub>2</sub> emission moderately.

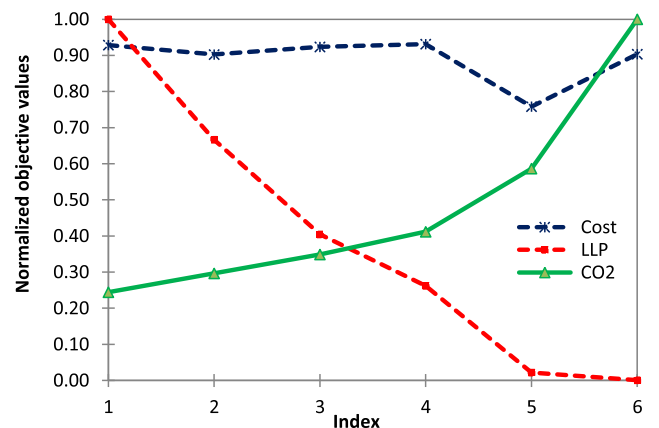


Fig. 15. Pruned solutions when CO<sub>2</sub> objective function is preferred.

**Table 3**  
Optimal size of components.

		PV (kw)	Wind (kw)	Diesel (kw)	Fuel cell (kw)	Battery (kwh)	Electrolyzer (kw)	H <sub>2</sub> -tank (kg)
Case 1	Proposed approach	8	6.5	1.8	0	66.4	0	0
	SPEA [21]	8	6.5	1.9	0	88.7	0	0
Case 2	Proposed approach	8	6.5	3.9	0	45.9	0	0
	SPEA [21]	8	6.5	4	0	44.3	0	0
Case 3	Proposed approach	8	6.5	3	0.11	88.7	1.1	4.2
	SPEA [21]	8	6.5	3	3	88.7	4	10

The Pareto front contains a large number of non-dominated points. Selecting a solution from such a large set is potentially difficult for a decision maker. In this study, the post-Pareto analysis is done for these 50 solutions, to provide the decision maker a workable sub-set of the solutions. The Post-Pareto analysis aids decision makers in choosing a single solution from a potentially large set of Pareto front. To find a representative subset of the solution set, first the objective values are normalized based on their maximum value among all non-dominated solutions. Six clusters are considered and the non-dominated solutions are distributed in these clusters such that objectives within the same cluster have a high degree of similarity. For distributing the solutions in the clusters, three cases are considered, in the first case the non-dominated solutions are ranked based on the normalized cost, and then a cluster is assigned to each solution regarding its normalized cost. The best ranked solution in each cluster is selected and shown in Fig. 13. Similarly, in the second case and the last one the solutions are ranked based on the normalized LLP and normalized CO<sub>2</sub>, respectively. In these cases the best solution of each cluster is also depicted in Fig. 14 and Fig. 15 respectively. In Figs. 13–15 each line describes an objective function, and each index is devoted to a solution. The index 1 stands for the solution with the best rank based on the normalized objective function, while index 6 stands for the worst one.

For comparing the results of the SPEA approach by Ref. [21] with the proposed approach, three cases which are mentioned in details by Ref. [21] are used. In these cases the desirable level for CO<sub>2</sub> emission and LLP are defined. In case 1:  $\epsilon_{LLP}=4.5\%$ ,  $\epsilon_{CO_2} = 1351$  kg/yr, in case 2:  $\epsilon_{LLP} = 0.5\%$ ,  $\epsilon_{CO_2} = 2421$  kg/yr, finally in case 3:  $\epsilon_{LLP}$  and are set as 1.8% and 1778 kg/yr, respectively. For these cases, the proposed approach is used to minimize the total cost of the system. The optimal size of the components and the corresponding total cost are presented in Table 3 and Fig. 16. It is noteworthy to mention that in this study the rectifiers cost, inverters and batteries charge regulator costs are neglected since the optimal sizing of these components is not considered. The result shows little contribution of hydrogen storage. One reason for this fact can be that hydrogen storage device is more expensive. In addition, the maximum overall energy efficiency of hydrogen storage device is resulted 28.9% which is less than battery overall energy efficiency (80%).

Dufo et al. [21] utilized discrete values for decision variables while the proposed approach deals with continuous optimization

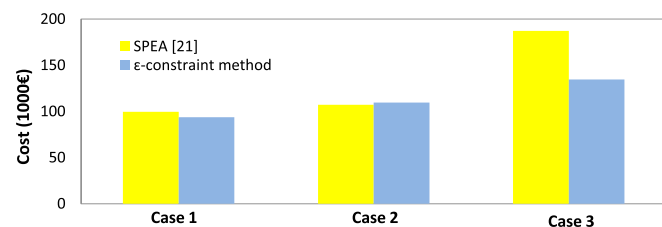


**Fig. 16.** Optimal costs using the  $\epsilon$ -constraint method and SPEA [21].

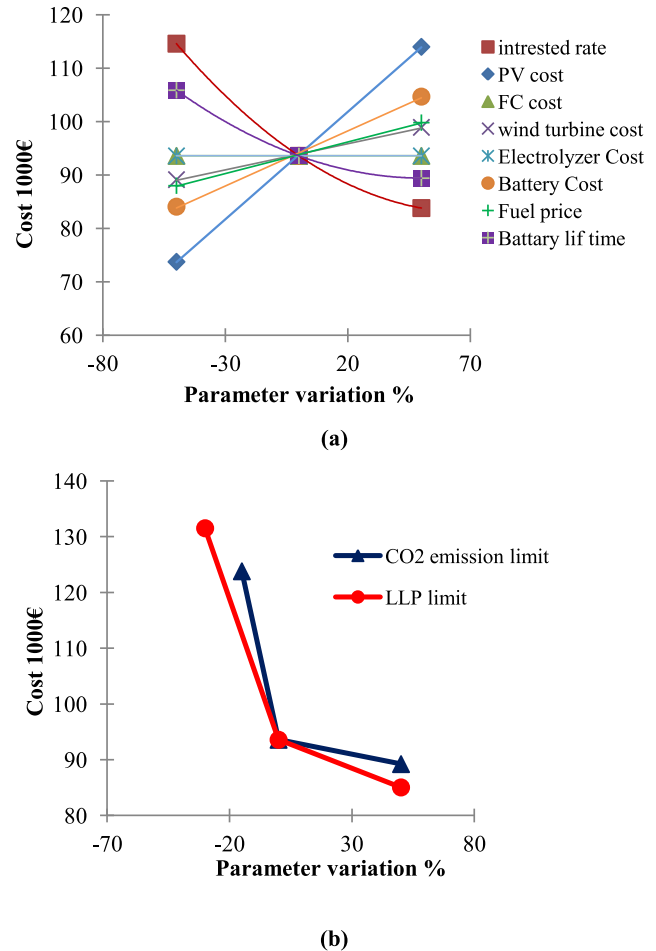


**Fig. 17.** Sensitivity analysis result.

problem; Hence, this fact can explain a slight difference between the proposed model results and Dufo et al. [19] results in cases 1 and 2. As shown in Fig. 16, it is observed that in the case 3 the  $\epsilon$ -constraint method yield a better cost (27% less) than SPEA results.

Sensitivity analysis is the investigation of how possible variation of the input parameters may impact the optimal solution provided by the optimization algorithm under a given set of assumptions [33]. In a sensitivity analysis, the values of parameters or inputs are changed and the resulted changes in performance indices are measured. Therefore, a main goal of a sensitivity analysis is to identify which parameters are the most sensitive and most likely to affect system behavior [33]. In this study, a sensitivity analysis is performed to investigate the effect of the input parameters on the optimal solution provided by the proposed approach in the case 1, if the parameters take other possible values. The considered parameters are the interest rate, PV panel capital cost, fuel cell capital cost, wind turbine capital cost, electrolyzer capital cost, battery capital cost, fuel price, battery life time, CO<sub>2</sub> emission and LLP allowable level. The sensitivity analysis results of case 1 are shown in Fig. 17. The optimal solution for the case result in the total cost 93,587 € for 25 years. The annual energy delivered to the load is 13,407 kWh and the gas oil consumption is 562 lit/year. By creating 20 additional scenarios:

- 50% Increase scenarios for following parameters: interest rate, PV panel capital cost, fuel cell capital cost, wind turbine capital cost, electrolyzer capital cost, battery capital cost, fuel price, battery life time, CO<sub>2</sub> emission and LLP allowable level.



- 50% decrease on following parameters: interest rate, PV panel capital cost, fuel cell capital cost, wind turbine capital cost, electrolyzer capital cost, battery capital cost, fuel price, battery life time, 15% decrease on CO<sub>2</sub> emission allowable level, and 30% decrease on LLP allowable level.

The optimal configuration is remained unchanged in the 16 scenarios which are 50% increase and 50% decrease scenarios for interest rate, PV panel capital cost, fuel cell capital cost, wind turbines capital cost, electrolyzer capital cost, battery capital cost, fuel price, and battery life time. A PV/wind turbine/battery/diesel system is resulted as the optimal configuration in these scenarios. The total cost approximately increases or decreases with the changes in these parameters while the components configurations are same, Fig. 17(a).

With 50% increase in allowable level for LLP and CO<sub>2</sub> emission, the optimal configuration do not change. As it is obvious from the result, there is a reduction in the total cost of the HRES since the optimal value of decision variables decrease, Table 2. As these allowable levels decrease 50%, the current solution becomes infeasible. Fig. 17 (b) shows that the total cost significantly increased when the LLP and CO<sub>2</sub> emission allowable levels decrease 30% and 15%, respectively. The result indicates that in these two scenarios, the optimal configuration is changed because satisfying the model constraints needs storing energy in hydrogen tank and using fuel cell and electrolyzer which are much inefficient than storing energy in batteries.

## 7. Conclusion

In this study, we present a novel approach for optimizing the size of a hybrid renewable energy system. The  $\epsilon$ -constraint method has been applied to minimize three objectives: loss of load probability, CO<sub>2</sub> emission, and the total cost of the system. The proposed approach used a PSO-simulation based method to solve the multi-objective optimization problem. The main advantage of the proposed approach is its simplicity which leads to computational efficiency.

In a case study including wind turbine, PV panels, diesel generator, fuel cell, electrolyzer, batteries and hydrogen tank the proposed approach is evaluated. By comparing the proposed approach results with the previous methods results, it has been concluded that an improvement in the total cost is obtained while achieving same fuel emission and LLP. A sensitivity analysis study is performed to study the sensibility of the input parameters to the developed model. The sensitivity analysis indicates that if the life time of the batteries and interest rate are reduced, the total cost increases. Furthermore, the total cost of the system is more sensitive to the allowable level of CO<sub>2</sub> emission compared to the other variables. The proposed model can be used in feasibility studies and the design of a HRES.

For future research, a detailed load analysis that takes into consideration the heat and electricity loads separately and load shifting will be performed to recommend an optimum system configuration that matches the load. In addition, uncertainty of the renewable energy sources availability and will also be taken into account.

## References

- [1] Dufo-Lopez R, Bernal-Augustin JL, Contreras J. Optimization of control strategies for stand-alone renewable energy systems with hydrogen storage. *Renew Energy* 2007;32(7):1102–26.
- [2] Qinghai B. Analysis of particle swarm optimization algorithm. *Comput Inform Sci* 2010;3(1):180–4.
- [3] Eke R, Kara O, Ulgen K. Optimization of a wind/PV hybrid power generation system. *Int J Green Energy* 2005;2(1):57–63.
- [4] Ludwig K, Bo Z, Grisselle C, Zhixin M. Stochastic optimization for power system configuration with renewable energy in remote areas. *Annu Operat Res* 2012;195:1–22.
- [5] Garyfallos G, Athanasios IP, Panos S, Spyros V. Optimum design and operation under uncertainty of power systems using renewable energy sources and hydrogen storage. *Hydrog Energy* 2010;35(3):872–89.
- [6] Akella AK, Sharma MP, Saini RP. Optimum utilization of renewable energy sources in a remote area. *Renew Sustain Energy Rev* 2007;11(5):894–908.
- [7] Hanane D, Ahmed O, Roberto S. Modeling and control of hydrogen and energy flows in a network of green hydrogen refueling stations powered by mixed renewable energy systems. *Hydrog Energy* 2012;37(6):5360–71.
- [8] Cai YP, Huang GH, Tana Q, Yang ZF. Planning of community-scale renewable energy management systems in a mixed stochastic and fuzzy environment. *Renew Energy* 2009;34(7):1833–47.
- [9] Jeremy L, Marcelo GS, Abdellatif M, Philippe C. Energy cost analysis of a solar-hydrogen hybrid energy system for stand-alone applications. *Hydrog Energy* 2008;33(12):2871–9.
- [10] Orhan E, Banu YE. Size optimization of a PV/wind hybrid energy conversion system with battery storage using simulated annealing. *Appl Energy* 2010;87(2):592–8.
- [11] Kashefi A, Riahy GH, Kouhsari SM. Optimal design of a reliable hydrogen-based stand-alone wind/PV generating system, considering component outages. *Renew Energy* 2009;34(11):2380–90.
- [12] Raquel SG, Daniel W. A wind–diesel system with hydrogen storage: joint optimization of design and dispatch. *Renew Energy* 2006;31(14):2296–320.
- [13] Iniyan S, Suganthi L, Anand AS. Energy models for commercial energy prediction and substitution of renewable energy sources. *Energy Policy* 2006;34(17):2640–53.
- [14] Juhari AR, Kamaruzzaman S, Yusoff A. Optimization of renewable Energy hybrid system by minimizing excess capacity. *Int J Energy* 2007;3(1):77–81.
- [15] Katsigiannis YA, Georgilakis PS. Optimal sizing of small isolated hybrid power systems using Tabu search. *Optoelectron Adv Mater* 2008;10(5):1241–5.
- [16] Budischak C, Sewell DA, Thomson H, Mach L, Veron DE, Kempton W. Cost-minimized combinations of wind power, solar power and electrochemical storage, powering the grid up to 99.9% of the time. *J Power Sources* 2013;225: 60–74.
- [17] Elliston B, MacGill I, Diesendorf M. Least cost 100% renewable electricity scenarios in the Australian National Electricity Market. *Energy Policy* 2013;59: 270–82.
- [18] Banos R, Manzano F, Montoya FG. Optimization methods applied to renewable and sustainable energy: a review. *Renew Sustain Energy Rev* 2011;15(4): 1753–66.
- [19] Katsigiannis YA, Georgilakis PS, Karapidakis ES. Multi objective genetic algorithm solution to the optimum economic and environmental performance problem of small autonomous hybrid power systems with renewable. *IET Renew Power Gener* 2010;4(5):404–19.
- [20] Trivedi M. Multi-objective generation scheduling with hybrid energy. PhD Dissertation. USA: Department of Electrical Engineering, Clemson University; 2007.
- [21] Rodolfo DL, Jose LBA. Multi-objective design of PV–wind–diesel–hydrogen–battery systems. *Renew Energy* 2008;33(12):2559–72.
- [22] Abedi S, Alimardani A, Ghahrepetian GB, Riahy GH, Hosseini SH. A comprehensive method for optimal power management and design of hybrid RES-based autonomous energy systems. *Renew Sustain Energy Rev* 2012;16(3):1577–87.
- [23] Jose LBA, Rodolfo DL. Efficient design of hybrid renewable energy systems using evolutionary algorithms. *Energy Convers Manag* 2009;50(3):479–89.
- [24] Ganguly A, Misra D, Ghosh S. Modeling and analysis of solar photovoltaic-electrolyzer-fuel cell hybrid power system integrated with a floriculture greenhouse. *Energy Build* 2010;42(11):2036–43.
- [25] Kaveh KD, Amir-Reza A, Madjid T. A new multi-objective particle swarm optimization method for solving reliability redundancy allocation problems. *Reliab Eng Syst Saf* 2013;111:58–75.
- [26] Coello CC, Lamont GB, Van-Veldhuizen DA. Evolutionary algorithms for solving multi-objective problems. 2nd ed. New York: Springer; 2007.
- [27] Hazem A, Janice G. Swarm intelligence: concepts, models and applications. Technical Report. Canada: School of Computing, Queen's University; 2012.
- [28] Swagatam D, Ajith A, Amit K. Particle swarm optimization and differential evolution algorithms: technical analysis, applications and hybridization perspectives. *Stud Comput Intell (SCI)* 2008;116:1–38.
- [29] Ahmarinezhad A, Abbaspour-Tehrani-fard A, Ehsan M, Fotuhi-Firuzabad M. Optimal sizing of a stand alone hybrid system for Ardabil area of Iran. *IJTPE* 2012;4(12):118–25.
- [30] Ranjithan SR, Chetan SK, Dakshina HK. Constraint method-based evolutionary algorithm (CMEA) for multiobjective optimization. *Lect Notes Comput Sci (LNCS)* 2001;1993:299–313.
- [31] Francisco G. Design optimization of stand-alone hybrid Energy systems. Msc thesis. University of Porto, Portugal; 2010.
- [32] Da-Rosa AV. Fundamentals of renewable energy processes. 2nd ed. Elsevier Academic Press; 2009.
- [33] Frederick SH, Gerald JL. Introduction to operations research. 9th ed. New York: Mc Graw Hill; 2010.